Slater and Takagi defects in KH_2PO_4 from first principles

J. Lasave,[1] S. Koval,[1,*] N. S. Dalal,[2] and R. Migoni[1]
[1]*Instituto de Física Rosario, Universidad Nacional de Rosario, 27 de Febrero 210 Bis, 2000 Rosario, Argentina*
[2]*Department of Chemistry and NHMFL, Florida State University, Tallahassee, Florida 32306, USA*
(Received 5 April 2005; revised manuscript received 1 June 2005; published 9 September 2005)

We performed *ab initio* electronic structure calculations to study the stability of the Slater and Takagi protonic defects in the ferroelectric phase of KH_2PO_4. We show that the Slater defects are stabilized only when they are aligned forming chains of defects in the lattice, in accordance with the *displacive model* of the transition. In contrast, the Takagi defects are not stable in the lattice. The *ab initio* energy estimation for the Takagi defect ($\approx$54 meV) is in fair good agreement with previous phenomenological estimates. However, the calculated *uncorrelated* Slater defect energy ($\approx$17 meV) is larger than that from previous model assignments (5.2 meV), while the latter agrees well with our result for the correlated value per formula unit. This suggests that the earlier estimates contain considerable contribution from correlations between configurations of different H_2PO_4 groups. Our *ab initio* results show that the formation of chains of Slater defects is accompanied by phosphate rotations, and a concomitant lattice contraction in the basal plane. Therefore, we propose that the as yet unexplained anomalous lattice contraction observed in the neighborhood of the phase transition is due to an increase of the Slater defect population.

DOI: 10.1103/PhysRevB.72.104104 PACS number(s): 77.84.Fa, 71.15.Nc, 77.80.−e

I. INTRODUCTION

Potassium dihydrogen phosphate (KH_2PO_4, or KDP), is the prototype of the hydrogen-bonded ferroelectric compounds. It has been the subject of intensive experimental and theoretical studies since the discovery of its ferroelectric transition at 123 K in 1935.[1] Despite considerable progress since then, a complete understanding of the ferroelectric transition mechanism is still lacking.

From the theoretical side, the first successful model of the KDP phase transition was developed by Slater in 1941.[2] In the Slater model, the ice rules are applied, and only two protons are allowed to be close to each phosphate in six possible configurations (Fig. 1). The lowest-energy configurations are the polar ones [see Fig. 1(a)], with electric dipoles pointing along the z direction, which characterize the low-temperature ferroelectric phase, with a net spontaneous polarization along this direction. The two polar configurations are built with protons attached to the bottom or the top oxygens in the phosphate, and differ in the sign of the corresponding dipoles along z. The remaining four configurations are the ones (hereafter called "Slater") where the two protons are laterally attached, respectively, to two oxygens, one at the top and the other at the bottom of the phosphate units [Fig. 1(b)]. These configurations have a higher energy ϵ_S (Slater energy) compared to that of the polar configurations in the ferroelectric phosphates. The Slater model predicts a sharp first-order ferroelectric transition, but because it is a static model in its original form, it is difficult to use it for understanding, in particular, dynamic properties, such as electric transport properties, and related protonic hopping in the low-temperature ferroelectric phase.[3]

Takagi improved the theory by including the possibility of configurations with one or three protons attached to the phosphate (Takagi configurations) with energy ϵ_T per phosphate above that of the polar configurations.[4] These configurations violate the ice rules and arise, e.g., when a proton from a H bond common to two polar states moves to the other bond side. This leads to the formation of a Takagi-pair defect with energy $2\epsilon_T$ in two neighboring phosphates that finally remain with one and three protons [see Fig. 1(c)].

Later improvements of these order-disorder models came with the addition of long-range interactions[5,6] and the introduction of tunneling[7] to account for the huge $H \leftrightarrow D$ isotope effect observed: Upon $H \rightarrow D$ substitution, the T_c increases from 123 to 224 K. Models that include proton-lattice interactions, and hence may display displacive features of the transition, were first introduced by Kobayashi.[8] Actually, strong evidence that the transition involves a displacive component with electronic instabilities was recently detected by nuclear magnetic resonance (NMR) experiments for $KD_{1.8}PO_4$ (Ref. 9) and squaric acid.[10] Particularly, in the

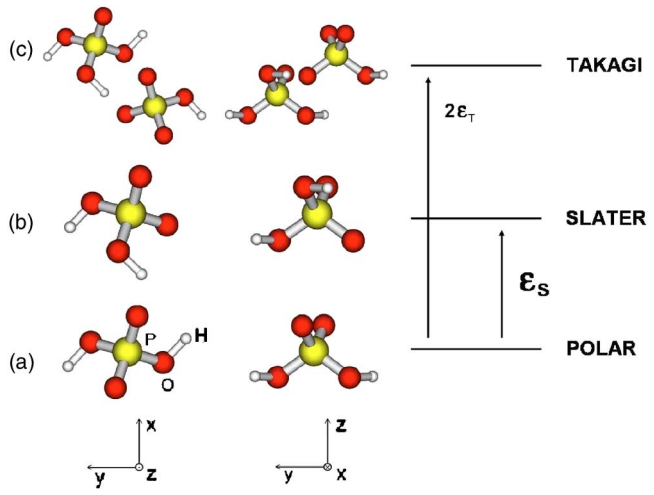

FIG. 1. (Color online) Different proton configurations for the phosphates in KDP: (a) Polar, (b) Slater, and (c) Takagi-pair defect. Left: Top view. Right: Frontal view. ϵ_S and $2\epsilon_T$ are the energies of the formation of a Slater and a Takagi-pair defect, respectively.

latter case, the coexistence of order-disorder and displacive features appear to be present near the phase transition.

Recent high-resolution neutron diffraction experiments provided evidence that the structural modifications in the hydrogen bond geometry are strongly correlated with the order parameter.[11,12] In this regard, these experiments show that, in the paraelectric phase, the distance δ between the two stable minima of the proton in the H bond is strongly correlated with T_c. It is also argued that the origin of the isotope effect is the geometric effect and not the tunneling itself, and that the proton and the host are definitively not separable systems.[13]

Phenomenological models were also proposed recently to take into account the geometrical effects with some success.[10,14–17] However, such model parametrizations are not always reliable regarding the physical meaning of the parameter values and their transferability upon structural or chemical changes.

Earlier magnetic resonance studies of DKDP (KD_2PO_4) showed the existence of deuteron jumping between H bonds, that is consistent with the Slater–Takagi theory of defects.[18] The domain-wall motion near the transition in DKDP was explained in terms of the effective motion of Takagi groups, leaving behind a string of Slater defects.[19] The slow motion of domain walls is also believed to be the cause of an anomaly in the dielectric constant of KDP as a function of temperature, which shows a plateau region immediately below T_c. The sudden fall of the plateaulike anomaly at $T_F \approx T_c - 60$ K is described as a "kink" and is related to the freezing of the domain-wall motion.[20] The stability and motion of thin domain walls was recently described by a Slater–Takagi model which also includes interactions between protons in parallel bonds.[21]

The Slater and Takagi energies (Fig. 1) were deduced earlier using phenomenological models (hydrogen-bond occupation models) that were fitted to the experimentally determined polarization curves in DKDP.[6] In the model of Ref. 6, the original Slater–Takagi model that takes into account the short-range interactions between protons in the same phosphate, was extended to include also long-range interactions with protons in neighboring phosphates. A good fit to the polarization curves was achieved for DKDP, although the calculated entropy was nearly twice that found in specific-heat experiments.[6] This discrepancy was corrected by Blinc and Svetina with the incorporation of the tunneling effects to this extended model.[22] They determined the Slater–Takagi energies of the different proton configurations around a given phosphate by integrating out all internal coordinates in a given PO_4 group. Using a different fitting procedure, but including also quantum effects from a small-tunneling approximation, Fairall and Reese tabulated the parameters of the hydrogen-bond occupation (order-disorder) model for various members of the KDP-type family.[3,23]

Ab initio calculations were conducted only very recently in KDP.[24–31] It was found that significant instabilities arise only when protons are allowed to relax together with heavy ions.[25–27] The huge deuteration isotope effect is shown to arise due to a self-consistent coupling, via modifications of the H-bridge covalency, between tunneling and the geometrical effects, thus dramatically enhancing the latter.[25] These results are in agreement with neutron diffraction,[11,12] Compton scattering,[32] and electron-nuclear double resonance (ENDOR) measurements performed recently.[33]

However, despite the evident importance of proton configurational defects in the dynamical behavior of these materials, their energies and stabilities have been estimated so far only at a rather phenomenological level. To our best knowledge, no *ab initio* calculations have been carried out to study the Slater or Takagi defects in H-bonded systems. In this work, we investigate the stability of different proton configurations by means of *ab initio* calculations within the density functional theory (DFT). Details of the *ab initio* method and the calculations are presented in Sec. II. In Sec. III, we analyze the results obtained and finally, we discuss and elaborate our conclusions in Sec. IV.

II. *AB INITIO* METHOD AND COMPUTATIONAL DETAILS

The first-principles calculation were carried out using the SIESTA program,[34] which is a fully self-consistent approach that employs a linear combination of confined pseudoatomic orbitals (PAO) of the Sankey–Niklevsky type as basis functions for the valence electrons.[35] We have chosen a double-zeta basis set with polarization functions (DZP) for these orbitals. The interaction between ionic cores and valence electrons is represented by angular-dependent norm-conserving pseudopotentials of the Troullier–Martins type.[36] Due to the large overlap between core and valence charge densities, we have also included nonlinear core corrections (NLCC) for a proper description of the K ion. Exchange-correlation energy functionals are computed within the gradient-corrected Perdew–Burke–Ernserhof (PBE) approximation.[37]

The grid computation of the numerical integrals was carried out with an energy cutoff of 125 Ry. The orbital confinement energy E_c, which measures the degree of approximation of the confined PAO,[34] is set to 50 meV, which gives total energies and geometries of sufficient accuracy. These approximations were also tested against results from standard pseudopotential plane-wave calculations.[24,25,27] The electronic Brillouin-zone sampling is reduced to the Γ-point, which proved to be a good approximation due to the large supercells used in the calculation.[25]

The ferroelectric (FE) phase structure in KDP is described with the conventional face-centered-tetragonal (fct) cell, containing 8 formula units (64 atoms), and axes rotated through 45° with respect to the conventional body-centered-tetragonal (bct) cell. A schematic view of the FE structure from the top (projection on the *xy* plane) is shown in Fig. 2(a). In this phase, two hydrogens are covalently attached to each phosphate in the polar configuration [see Fig. 1(a)], which has the lowest possible energy.

The main calculations were carried out with the cell parameters fixed at the experimental values at $T = T_c^{\mathrm{KDP}} - 20$ K for KDP, which is orthorhombic.[38] After relaxing all of the atoms in this cell, we obtained the FE (polar) phase as depicted in Fig. 2(a), with internal parameters in general good agreement with experiments.[24,25,31]

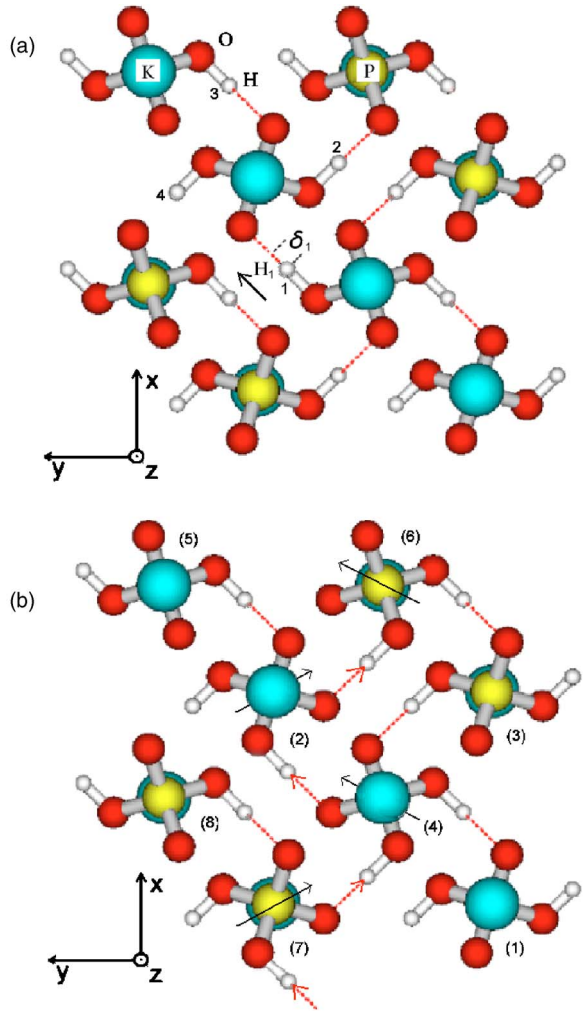

FIG. 2. (Color online) Conventional fct cell of KDP from a top view showing: (a) The FE phase, where each phosphate is in the polar configuration (P structure). The arrow shows the direction of the reference H_1 shift to produce a Takagi pair. The labeling of the four H bonds surrounding one of the phosphates is indicated. δ_1 is the distance between positions, equidistant from the middle of the reference O–H–O bond labeled by 1. (b) Formation of a chain of four Slater defects connected through periodic boundary conditions (S structure). Dashed arrows indicate the direction of hydrogen motion to form the chain. Solid arrows show the dipole moments developed by each phosphate in Slater configuration, which point approximately in the *xy* plane. The labels assigned to each of the phosphates in the cell are in brackets.

In order to study the formation of configurational defects involving local distortions of the polar state, we define the magnitude K_δ^i for each phosphate as follows:

$$K_\delta^i = \left| \frac{\delta_1^i + \delta_3^i - \delta_2^i - \delta_4^i}{2\delta_1} \right|, \qquad (1)$$

where δ_j^i is the δ value corresponding to the jth H bond ($j=1$–4) connecting the ith phosphate of the fct cell ($i=1$–8) with its neighbors [see Fig. 2(a)]. δ_j^i is considered to be negative if the corresponding H lies on the ith phosphate side of the jth bond, and positive otherwise. δ_1 is the δ value at a reference bond where the hydrogen is moved by constraining it at different positions along the bond in order to create the defect. In the case of formation of polar, Takagi, and Slater configurations (see Fig. 1), K_δ^i will approximately assume the values of 2, 1, and 0, respectively.

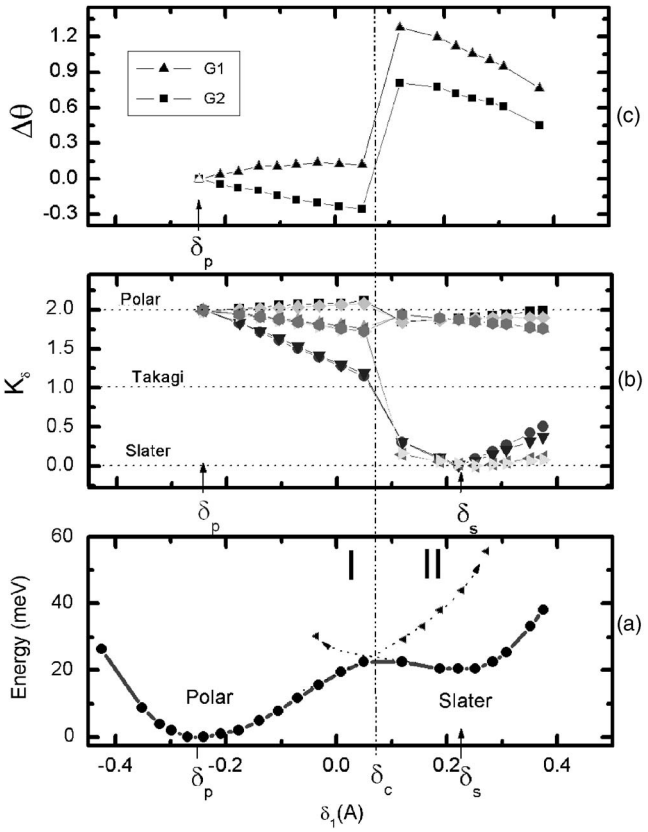

FIG. 3. (a) Total energy as a function of the hydrogen displacement δ_1 in the reference bond (solid curve and circles). Dashed lines and small left-triangle symbols correspond to the higher-energy continuation of the Slater and polar energy curves. (b) Proton arrangement factor K_δ as a function of δ_1. Different symbols and lines correspond to the eight different phosphates in the conventional cell. (c) Variation of the angle parameter θ with respect to the polar state, averaged over the group of phosphates $G_1=(8,5,6,4)$ (triangles) and $G_2=(7,2,3,1)$ (squares) [see Fig. 2(b) for the labels assigned to the phosphates]. $\Delta\theta$ is in degrees. Lines are only a guide for the eyes.

III. RESULTS

A. Stability of defects

We first explore the possibility of formation of a Takagi-pair defect [see Fig. 1(c)]. To this purpose, the hydrogen H_1 of a reference H bond is moved in the direction of the arrow [see Fig. 2(a)] toward the opposite side of the bond, and its position is constrained at different values of δ_1 in the polar phase (P structure). All of the remaining atoms of the cell are allowed to relax in such a way that the computed total energy is minimized.

In Fig. 3(a), we show the energy as a function of the hydrogen H_1 displacement (solid curve). As the hydrogen

leaves the equilibrium position for the P structure ($\delta_1 \approx -0.24$ Å $\equiv \delta_P$), the energy increases. However, after surpassing the middle of the H bond ($\delta_1 \approx 0.07$ Å $\equiv \delta_c$), the energy starts to decrease. In fact, on the other side of the equilibrium position along the bond, there appears another minimum of the total energy at $\delta_1 = +0.23$ Å $\equiv \delta_S \approx -\delta_P$. For values of $\delta > \delta_S$, as the H moves further away from the latter minimum and approaches the opposite oxygen, the energy increases again.

We show in Fig. 3(b) the parameter K_δ^i as a function of δ_1 for each of the eight phosphates in the conventional fct cell used. As the hydrogen H_1 is shifted toward the middle of the bond, we observe the tendency of the system to form a Takagi pair. Particularly, at $\delta_1 = \delta_c$, K_δ assumes a value of ≈ 1 for the pair of phosphates connected by the hydrogen H_1. Nearest-neighbor hydrogens are also strongly perturbed at this stage, and their positions are shifted with respect to those in the polar phase as is seen in Fig. 3(b), which is a consequence of the strong correlations among ionic displacements.[25] We will see below that this has its origin in phosphate rotations coupled to the H motion.

With increasing H_1 displacement, we observe at $\delta_1 = \delta_c$ a sudden change of configuration for one-half of the phosphates in the cell, indicated by their values of $K_\delta \approx 0$ for $\delta_1 > \delta_c$ [see Fig. 3(b)]. Moreover, the energy minimum seen in Fig. 3(a) at $\delta_1 = \delta_S$, corresponds to these four phosphates in Slater configuration ($K_\delta \approx 0$), while the other phosphates remain in polar configurations ($K_\delta \approx 2$). The four phosphates in the Slater configuration are linked and build a chain, which is extended to infinity through periodic boundary conditions. We call this configuration, depicted in Fig. 2(b), the S structure. In the polar P phase, all of the dipole moments point along the ferroelectric z axis [see Fig. 2(a)]. The formation of Slater defects in the S structure leads to a change of the dipole-moment directions, which turn perpendicular to the z axis in the affected phosphates [see solid arrows in Fig. 2(b)], while Takagi-pair defects do not appear in this structure. In fact, the positioning of the H_1 at the opposite side of the reference bond produces a concomitant displacement of other three hydrogens in the directions of the dotted arrows, as shown in Fig. 2(b). These H motions are strongly correlated and the energy is minimized by the formation of a chain of Slater defects.

It is possible that S structures with finite length are stable, the correlation length being larger than the size of the fct cell used with periodic boundary conditions. In such a case, the S structure should end with Takagi defects. Unfortunately, our computer capability does not allow us to consider larger cells. For further verification of the correlations among Slater defects, we have also studied the stability of the defects chain while constraining any one of these hydrogens to remain fixed at its original position in the polar phase. In this case, the correlated displacement is aborted due to the fact that it would lead to the formation of a Takagi pair within the chain, which demands much more energy than the formation of the infinite chain. We want to stress here, that if we further relax the reference hydrogen from its position at δ_S, together with all atoms in the S structure, we again obtain approximately the same chain of Slater defects with a slightly smaller energy, by about 2 meV, than that shown in Fig. 3(a). Hence, our conclusions do not change significantly if we relax the constraint imposed, which is however necessary to obtain the whole curves of Fig. 3, and not just the results at the minima.

In addition to the minimum corresponding to Slater defects for $\delta_1 > \delta_c$ (Region II), we found around δ_S other locally stable configurations with higher energy. These configurations resemble those found in region I corresponding to the Takagi-pair formation, and lie on the continuation of the minimum-energy curve as is shown by small triangle symbols and dotted lines in Region II of Fig. 3(a). A small activation barrier connects these higher-energy states with the minimum-energy S structures shown by the solid curve in Region II of Fig. 3(a). Conversely, for $\delta_1 < \delta_c$ (Region I), we found higher-energy configurations resembling those with Slater defects of Region II, which are also shown as dotted lines and small triangle symbols [Fig. 3(a)] and are a continuation of the minimum-energy curve of Region II into Region I.

Summarizing, we clearly observe two different regions in Fig. 3(a): One for $\delta_1 < \delta_c$ where the Takagi-pair formation takes place, and the other for $\delta_1 > \delta_c$ characterized by the formation of Slater defects chains (S structures).

B. Energy of Slater and Takagi defects

We now discuss our *ab initio* study of the Slater–Takagi energy parameters, ϵ_S and ϵ_T. As we already mentioned, a Takagi-pair defect alone is not stable in the lattice (see Fig. 3). However, we may estimate its energy, $2\epsilon_T$, by constraining the reference hydrogen H_1 to lie on the opposite side ($\delta_1 = -\delta_P$) in the FE phase [Fig. 2(a)]. The oxygens and the remaining hydrogen atoms are fixed in their positions in this phase, and only the P and K atoms are allowed to relax. In this way, we are not including the effect of correlations between H_1 and the other hydrogens in the lattice, which are part of the long-range interactions.[22]

For the calculation of the Slater energy, ϵ_S, we moved H_1 and H_2 [see Fig. 2(a)], fixed them at the opposite side of the corresponding H bonds in the polar phase, and relaxed the P and K atomic positions. Thus, we created two Takagi defects and a Slater defect at the middle of three neighboring phosphates. We computed its energy E_{S2T}, which together with the previously obtained value of ϵ_T allows us to determine ϵ_S:

$$\epsilon_S = E_{S2T} - 2\epsilon_T. \tag{2}$$

We have also determined for comparison the correlated Slater energy, which includes part of the long-range correlations, as $\epsilon_S^{\mathrm{corr}} = E_{\mathrm{tot}}(\delta_S)/4$. Here, $E_{\mathrm{tot}}(\delta_S)$ is the total *ab initio* energy at δ_S, where the chain of Slater defects becomes stable [see the minimum in Region II of Fig. 3(a)]. Interestingly, we have that $\delta_S \approx -\delta_P$. Similarly, a correlated Takagi energy $\epsilon_T^{\mathrm{corr}}$ is defined as the local-minimum energy at δ_S, represented by the dashed line in Region II of Fig. 3(a). In this case, we mean "correlated" in the sense that all atoms of the cell, except the H_1, are allowed to relax to their equilibrium positions.

TABLE I. *Ab initio* energy per phosphate in meV obtained for the different proton configurations studied in this work. Also shown for comparison are previous model results fitted to polarization curves in KDP.[a]

	Energy per phosphate (meV)	
Parameters	*Ab initio*	Model[a]
ϵ_T	53.5	60.9
ϵ_T^{corr}	25.0	
ϵ_S	16.9	5.2
ϵ_S^{corr}	5.0	

[a]See Ref. 23.

The calculated parameters are shown in Table I, together with results from a model derived to fit the polarization curve in KDP by Reese *et al.*[23] We find a Takagi energy similar to that derived by model calculations. However, we obtain a Slater energy substantially larger than that determined by the phenomenological calculations in Ref. 23. On the other hand, the correlated parameters $\epsilon_T^{\mathrm{corr}}$ and $\epsilon_S^{\mathrm{corr}}$ are, respectively, $\approx 1/2$ and $\approx 1/3$ those of the corresponding uncorrelated parameters, showing the existence of strong correlations in the system.[25] We notice that the correlated parameter $\epsilon_S^{\mathrm{corr}}$ approaches the value obtained by the Reese calculations (see Table I). This fact leads us to speculate that the Slater energy parameter involved in the earlier models[5,6,23] effectively contains a significant contribution of correlations.

C. Correlations among Slater defects and phosphate rotations

In the process of forming a chain of Slater defects, we observed other important structural changes. Besides the phosphate distortions which give rise to the dipole moments in the *xy* plane [see Fig. 2(b)], we have also found that the interphosphate O–O distances at δ_S shrink about 0.3% with respect to those of the polar phase at δ_P. If $\langle d_{\mathrm{OO}}\rangle^i$ is the average of the O–O distance between the oxygens in the *i*th phosphate and the oxygens linked to them in the neighboring phosphates, we have verified that $\langle d_{OO}\rangle^i(\delta_S) < \langle d_{OO}\rangle^i(\delta_P)$ for each phosphate in the cell. Therefore, since all interphosphate O–O distances decrease with respect to those of the polar phase approximately by the same amount at δ_S, we conclude that the appearance of an S structure is associated with a phosphate rotation around the *z* direction. To investigate this feature in more detail, we determined, for each phosphate, the smallest angle θ in clockwise sense from the *x* axis up to the projection onto the *xy* plane of a P–O bond (see Fig. 2). This angle defines the orientation of the phosphates around the *z* axis as in Ref. 38. Then, for each phosphate *i*, we computed as a function of δ_1 the difference $\Delta\theta^i$ in the rotation angle respect to the polar phase at δ_P:

$$\Delta\theta^i(\delta_1) = \theta^i(\delta_1) - \theta^i(\delta_P). \tag{3}$$

With δ_1 increasing from δ_P, we found that there are basically two phosphate groups G_1 and G_2, each having similar variations of phosphate rotation angles $\Delta\theta_1$ and $\Delta\theta_2$, respectively. The phosphates of a given group are on alternating *xz* planes along the *y* axis, i.e., G_1=8,5,6,4 and G_2=7,2,3,1 [see numbers in brackets identifying the phosphates in Fig. 2(b)]. For the sake of simplicity, let us consider the average rotation-angle variation for each phosphate group G (G_1 or G_2):

$$\Delta\theta^G(\delta_1) = \frac{1}{4}\left(\sum_{i\in G}\Delta\theta^i(\delta_1)\right). \tag{4}$$

In Fig. 3(c), we plot $\Delta\theta \equiv \Delta\theta^G(\delta_1)$ as a function of δ_1 for each group of phosphates, G_1 (triangles) and G_2 (squares).

As δ_1 increases and H_1 approaches the middle of the *j* =1 H bond, $\Delta\theta$ becomes increasingly negative for G_2 while it remains almost constant for G_1. This holds as long as $\delta_1 < \delta_c$, as observed in Fig. 3(c). Thus, while a Takagi-pair centered at H_1 is formed, the phosphates of G_2 linked to the H-donor phosphate [*i*=4, in Fig. 2(b)] rotate counterclockwise. This produces a shrinking of the O–O distances in the H bonds connected to the donor phosphate, which accounts for the strong correlations observed during the Takagi-pair formation (Region I in Fig. 3). Moreover, as $\delta \to \delta_c$, these rotations and the related O–O bond shrinking would favor the correlated proton hopping necessary to produce the chain of Slater defects observed in Region II. In fact, soon after $\delta > \delta_c$, a drastic change in the behavior of $\Delta\theta$ for both groups is observed. Both groups rotate clockwise more than one degree at δ_c, as shown in Fig. 3(c). These last rotations are concomitant with the correlated jumping of the four H's [see Fig. 2(b)], which leads to the S structure at δ_S, as observed in Figs. 3(b) and 3(c). Although both groups rotate in the same sense, the O–O contractions observed at δ_S are explained by the fact that $\Delta\theta^{G_1} > \Delta\theta^{G_2}$.

D. Thermal expansion anomaly

The contractions in all of the O–O distances found in the S structure, would in turn affect the crystal cohesion. We show in this section that this feature can be related to an anomalous lattice contraction observed as *T* increases approaching T_c in KDP and other related compounds.[39,40] To investigate this feature in detail, we relaxed the cell parameters and all atomic positions in both configurations studied in this work: (i) The P structure (FE phase), and (ii) the S structure [Figs. 2(a) and 2(b), respectively]. It is worth mentioning that the full relaxations do not alter the described characteristics of the P and S structures. Both relaxed cells are orthorhombic with cell parameters (a_P, b_P, c_P) and (a_S, b_S, c_S) for the P and S structures, respectively. To better compare the effect of the different structures in both cells, we define the pseudomonoclinic cell with parameters (a', γ, c), where $a' = \frac{1}{2}\sqrt{a^2+b^2}$ and $\gamma = 2\arcsin(b/\sqrt{a^2+b^2})$. Results from the relaxations are shown in Table II, together with experimental data from Ref. 39 at different *T* as they tend to $T_c \simeq 122$ K from the FE phase.

The relaxed FE cell is obtained in good agreement with experiment. The calculated S cell is contracted in the *xy* plane and elongated in the *z* direction approximately 0.1% relative to the relaxed cell of the FE phase. We also note that

TABLE II. *Ab initio* parameters of the pseudomonoclinic cell obtained by relaxation of the structures P and S. Also shown are the experimental parameters obtained by Kobayashi *et al.* at different temperatures approaching T_c.[a] Parameters a' and c are given in Å, and γ in degrees.

	Ab initio structures		Experimental data[a]		
Cell parameters	P	S	103.86 K	113.56 K	122.76 K (T_c)
a'	7.580	7.575	7.4290(7)	7.4290(7)	7.427(7)
γ	90.28	90.07	90.433	90.414	90.262
c	6.945	6.952	6.9264(7)	6.9272(7)	6.926

[a]See Ref. 39.

the parameter γ_S is about 0.3% smaller than γ_P. Moreover, γ_S is almost 90°, i.e., the S cell may be considered as nearly tetragonal, in contrast to the FE cell which is clearly orthorhombic (see Table II). The cell contraction in the xy plane is a consequence of the phosphate rotations and the concomitant O–O bond shrinking discussed in the previous subsection.

As was pointed out in Ref. 40, an anomalous contraction of the cell parameters a and b is observed experimentally when T increases tending to T_c in KDP. This anomaly was also observed in squaric acid and $PbHPO_4$. The experimental contraction in the xy plane is shown in Table II, in terms of the parameters a' and γ of the pseudomonoclinic cell. The contraction in these parameters is about 0.05–0.2% as T increases from T_c-20 K to T_c. It is also observed experimentally as $T\rightarrow T_c$ that the orthorhombicity of the cell tends to decrease, i.e., γ diminishes and approaches the value of 90° (see Table II).

The behavior of the unit cell parameter c in the region $\{T_c-20\ \mathrm{K}, T_c\}$ is somewhat different than that for the basal parameters. Actually, as shown in Table II, in the first part of this region, the parameter c grows and it finally experiments a contraction very near to T_c. As a result of this, the total cell volume experiences a final contraction as T_c is approached from the FE phase.

The existence of Slater defects near the transition in the paraelectric phase was inferred from the ^{75}As nuclear quadrupole resonance (NQR) experiments in KH_2AsO_4 and a family of related H-bonded arsenates.[41] Molecular dynamics simulations with a modified strong dipole-proton coupling model (MS-DPC) including Slater contributions[16] explained satisfactorily the NMR data of the ^{31}P nucleus in $KD_{1.8}H_{0.2}PO_4$ (Ref. 9) and the ^{75}As NQR data.[42] These calculations indicated also that the S-shaped anomaly in the T dependence of the local order parameter in KDP is related to the mentioned NQR data and that it originates from the change of population between polar and Slater configurations on approaching T_c. For instance, the sudden decrease of the local-order parameter found as T increases and approaches T_c, was correlated with the appearance of locally induced Slater configurations.[16]

The last discussion enables us to propose that the observed lattice contraction, in the xy plane as T grows and reaches T_c, can be explained in terms of the appearance of clusters of Slater defects in the lattice. At $T=0$ K, the system is in its FE ground state, but as T increases, chains of Slater defects within the S structure, which are locally stable, would have more statistical weight to effectively appear in the dynamics of the system. In fact, the barrier between the P and S configurations is of the order of $\epsilon_S^{\mathrm{corr}}\equiv E_{\mathrm{tot}}(\delta_S)/4$ per phosphate [see Fig. 3(a)], and hence, at temperatures around $T_S\equiv\epsilon_S^{\mathrm{corr}}/K_B\simeq 60$ K, finite-size clusters with the S structure would have a nonvanishing probability to coexist with P structure clusters in the lattice. Of course, quantum delocalization effects and thermal fluctuations would lead to an even smaller effective barrier between such configurations.[25,31] Then, the coexistence of Slater and polar configurations as $T\rightarrow T_c$ (note that $T_S\simeq 1/2T_c$) would in turn produce an increase in the probability of lattice contractions in the xy plane, due to the fact that the S structure exhibits smaller a' and γ parameters than the P structure. This fact qualitatively explains the lattice contractions in the basal plane and the tendency to a smaller orthorhombicity, observed experimentally as $T\rightarrow T_c$ (see Table II).

The appearance of Slater defects would also elongate the parameter c, which is in accordance with the experimental trend for this magnitude between 100 K and 115 K (Table II). On the other hand, our analysis cannot account for the final contraction observed in the parameter c very near to T_c, which might be related with an ultimate PO_4 reorientation produced dynamically near the phase transition.[40,43]

IV. DISCUSSIONS AND CONCLUSIONS

The existence of strings of Slater configurations created by the migration of Takagi defects was postulated several decades ago and shown to be consistent with deuteron NMR experiments.[19] These strings are visualized in phenomenological simulations, as part of domain walls responsible of the dielectric anomaly observed at the domain freezing temperature T_F.[21] Our *ab initio* calculations enable the formation of such nonpolar layers in KDP, giving further support to the results obtained in Ref. 21. According to our results, these layers would arise macroscopically in the lattice at temperatures around $T_S\approx 60$ K, in remarkable coincidence with T_F.

The problem of how the O-H$\cdots$O proton exchange takes place is a long pending issue.[41] Some experiments, e.g., Raman studies,[44] seem to indicate the importance of the H_2PO_4 order-disorder model, in which only the two up-down H_2PO_4 configurations of C_2 symmetry are involved. However, the ^{75}As NQR data seem to indicate that, besides the polar states, the Slater configurations (C_1 symmetry) also take part in the proton exchange.[42] Although the NQR experiments were not carried out on KDP itself, but on other compounds (KH_2AsO_4 and related materials), it is claimed that the C_1 configurations play also an important role in the KDP phase transition as well. Moreover, it is argued that the smaller statistical weight of the C_1 configurations and signal-to-noise problems in the scattering experiments are the origin of the absence of indications of these configurations in Raman measurements in KDP.[41]

Regarding this controversy we can say on the one hand, that strong correlations allow the existence of Slater defects

only as long line-defects. This is in favor of a displacive-like picture of the transition, as recently indicated by NMR measurements.[9] On the other hand, if we move a line of four hydrogens in one step [dashed arrows in Fig. 2(b)], and in each successive step we displace a neighboring H line in the xz plane in alternating directions along x, then after completing four steps in our cell, we change the polarization sense in the polar phase. We found that the largest barrier for each of the four steps is of the order of $4\epsilon_S^{\mathrm{corr}}$, which is much smaller than the barrier for the global polarization flip along z. This picture is in agreement with a model according to which the Slater configurations appear in the proton exchange,[41] as verified by the NQR data.[42] We conclude that in a scenario of larger simulation cells, with more than eight KH_2PO_4 units, the polarization flip would then take place in steplike form, with the formation of chains of Slater defects having a preponderant role. Moreover, this process would also be involved in the motion of domain walls.[21]

Raman spectra in the $x(yx)y$ configuration show a well-defined inelastic side peak (S peak) at about 145 cm^{-1}, in addition to the broad band in the central part, which appears when T is lowered below T_c.[45] The S peak has been traditionally assigned to the proton tunneling mode in KDP at $T < T_c$, although Raman measurements have discarded this assignment.[44] Actually, the S peak shows up in the $z(xy)\bar{z}$ spectrum of DKDP at a higher frequency than in KDP, and hence this mode was finally assigned to the libration mode of PO_4 tetrahedra, with A_1 symmetry.[44] However, it has been subsequently pointed out in Ref. 45 that the S peak cannot stem from a librational PO_4 mode, because this type of mode should not be affected by deuteration. We have shown in our calculations that the appearance of Slater defect chains is accompanied by phosphate rotations. The symmetry of these rotations is similar to that of the librational A_1 mode. The fact that Slater defects are induced near T_c,[42,16] and that they are coupled to phosphate rotations, as demonstrated in this work, may then explain why the librational mode is deuteration dependent. Moreover, this argument is further supported by the fact that the phosphate rotations induced by Slater defects finally lead to the lattice contraction observed experimentally near T_c,[39,40] as was discussed in the previous section. Interestingly, a strong coupling between the librational mode and the proton soft mode was observed recently in another *ab initio* calculation.[46]

Our calculations show that as H approaches the middle of the O–O bond, this bond contracts and the phosphates rotate. In a dynamical sense, it implies that this concerted motion would increase the hopping probability of the hydrogens between the two sides of the bond. We have shown in Fig. 3(c) that the hopping actually takes place at δ_c, and the phosphates rotate again to the other direction. We want to stress here that this phenomenon, although shown in a static simulation, should be related to a mechanism of assisted proton hopping. That is, protons may jump collectively to the other side of the bond, helped by phosphate rotations that lower the effective barrier for the H transfer.

In summary, we have shown by means of *ab initio* electronic structure calculations, that Slater defects are stabilized by their nucleation in chains in the FE phase of KDP, a fact that gives further support to the displacive picture of the transition. The uncorrelated Takagi energy parameter ($\approx$54 meV) is in good agreement with previous phenomenological estimates. In contrast, the corresponding Slater parameter ($\approx$17 meV) is larger in our calculation, while the correlated value per phosphate agrees well with the phenomenological estimates, suggesting that the latter include considerable effective correlations in their evaluation. We have also shown that the chain of Slater defects induces phosphate rotations, which in turn produce a lattice contraction in the xy plane. These results establish, for the first time, a connection between both phenomena, i.e., the appearance of Slater defects and the basal lattice contraction, which were observed independently in different experiments near Tc.[42,39]

ACKNOWLEDGMENTS

This work was supported in part by the Agencia Nacional de Promoción Científica y Tecnológica and CONICET under Grant No. PICT99 Nr. 03-07248. R.M. and S.K. acknowledge additional support from CONICET. S.K. acknowledges support from Florida State University (FSU), Tallahassee, USA, and also the kind hospitality received during the stay at the Department of Chemistry and Biochemistry of FSU. S.K. also acknowledges support from Fundación Antorchas, Argentina.

*Corresponding author. E-mail address: koval@ifir.edu.ar

[1] G. Busch and P. Scherrer, Naturwiss. **23**, 737 (1935).
[2] J. C. Slater, J. Chem. Phys. **9**, 16 (1941).
[3] V. H. Schmidt, Ferroelectrics **72**, 157 (1987).
[4] Y. Takagi, J. Phys. Soc. Jpn. **3**, 273 (1948).
[5] M. E. Senko, Phys. Rev. **121**, 1599 (1961).
[6] H. B. Silsbee, E. A. Uehling, and V. H. Schmidt, Phys. Rev. **133**, A165 (1964).
[7] R. Blinc, J. Phys. Chem. Solids **13**, 204 (1960).
[8] K. Kobayashi, J. Phys. Soc. Jpn. **24**, 497 (1968).
[9] A. Bussmann-Holder, N. Dalal, R. Fu, and R. Migoni, J. Phys.: Condens. Matter **13**, L231 (2001).
[10] N. Dalal, A. Klymachyov, and A. Bussmann-Holder, Phys. Rev. Lett. **81**, 5924 (1998).
[11] M. I. McMahon, R. J. Nelmes, W. F. Kuhs, R. Dorwarth, R. O. Piltz, and Z. Tun, Nature (London) **348**, 317 (1990).
[12] R. J. Nelmes, M. I. McMahon, R. O. Piltz, and N. G. Wright, Ferroelectrics **124**, 355 (1991).
[13] J. A. Krumhansl, Nature (London) **348**, 285 (1990).
[14] H. Sugimoto and S. Ikeda, Phys. Rev. Lett. **67**, 1306 (1991).
[15] A. Bussmann-Holder and K. H. Michel, Phys. Rev. Lett. **80**, 2173 (1998).
[16] D. Merunka and B. Rakvin, Solid State Commun. **129**, 375 (2004).

[17] D. Merunka and B. Rakvin, Chem. Phys. Lett. **393**, 558 (2004).
[18] V. H. Schmidt and E. A. Uehling, Phys. Rev. **126**, 447 (1962).
[19] V. H. Schmidt, Phys. Rev. **164**, 749 (1967).
[20] Y. N. Huang, X. Li, Y. Ding, Y. N. Wang, H. M. Shen, Z. F. Zhang, C. S. Fang, S. H. Zhuo, and P. C. W. Fung, Phys. Rev. B **55**, 16159 (1997).
[21] V. H. Schmidt, G. Bohannan, D. Arbogast, and G. Tuthill, J. Phys. Chem. Solids **61**, 283 (2000).
[22] R. Blinc and S. Svetina, Phys. Rev. **147**, 430 (1966).
[23] W. Reese, Phys. Rev. **181**, 905 (1969); C. W. Fairall and W. Reese, Phys. Rev. B **11**, 2066 (1975).
[24] S. Koval, J. Kohanoff, R. L. Migoni, and A. Bussmann-Holder, Comput. Mater. Sci. **22**, 87 (2001).
[25] S. Koval, J. Kohanoff, R. L. Migoni, and E. Tosatti, Phys. Rev. Lett. **89**, 187602 (2002).
[26] Q. Zhang, F. Chen, N. Kioussis, S. G. Demos, and H. B. Radousky, Phys. Rev. B **65**, 024108 (2001).
[27] S. Koval, J. Kohanoff, and R. L. Migoni, Ferroelectrics **268**, 239 (2002).
[28] C. S. Liu, N. Kioussis, S. G. Demos, and H. B. Radousky, Phys. Rev. Lett. **91**, 015505 (2003).
[29] C. S. Liu, Q. Zhang, N. Kioussis, S. G. Demos, and H. B. Radousky, Phys. Rev. B **68**, 224107 (2003).
[30] G. Colizzi, J. Kohanoff, J. Lasave, S. Koval, and R. L. Migoni, Ferroelectrics **301**, 61 (2004).
[31] S. Koval, J. Kohanoff, J. Lasave, G. Colizzi, and R. L. Migoni, Phys. Rev. B **71**, 184102 (2005).
[32] G. F. Reiter, J. Mayers, and P. Platzman, Phys. Rev. Lett. **89**, 135505 (2002).
[33] B. Rakvin and N. S. Dalal, Phys. Rev. B **44**, R892 (1991).
[34] P. Ordejón, E. Artacho, and J. M. Soler, Phys. Rev. B **53**, R10441 (1996); D. Sánchez-Portal, P. Ordejón, E. Artacho, and J. M. Soler, Int. J. Quantum Chem. **65**, 453 (1997).
[35] O. F. Sankey and D. J. Niklewski, Phys. Rev. B **40**, 3979 (1989).
[36] N. Troullier and J. L. Martins, Phys. Rev. B **43**, 1993 (1991).
[37] J. P. Perdew, K. Burke, and M. Ernzerhof, Phys. Rev. Lett. **77**, 3865 (1996).
[38] R. J. Nelmes, Z. Tun, and W. F. Kuhs, Ferroelectrics **71**, 125 (1987).
[39] J. Kobayashi, Y. Mesu, I. Mizutani, and Y. Enomoto, Phys. Status Solidi A **3**, 63 (1970).
[40] A. Katrusiak, Phys. Rev. B **48**, 2992 (1993).
[41] R. Blinc and B. Zeks, Ferroelectrics **72**, 193 (1987).
[42] R. Blinc and J. L. Bjorkstam, Phys. Rev. Lett. **23**, 788 (1969).
[43] M. Ichikawa, D. Amasaki, T. Gustafsson, and I. Olovsson, Phys. Rev. B **64**, R100101 (2001).
[44] Y. Tominaga, M. Kashara, H. Urabe, and I. Tatsuzaki, Solid State Commun. **47**, 835 (1983); Y. Tominaga, H. Urabe, and M. Tokunaga, *ibid.* **48**, 265 (1983).
[45] Y. Takagi, Ferroelectrics **72**, 67 (1987).
[46] G. Colizzi, Ph.D. thesis, Queen's University of Belfast, UK, 2004.